Position Alignment in 1995

Kirill Filimonov

McGill University, Foster Radiation Laboratory

3559 University, Montreal, Quebec, H3A 2B1

Version 2.0

(September 26, 1996)

Abstract

The position alignment of E877 tracking detectors is discussed. The correction factors are calculated for 1995 run. The preliminary proposed spectrometer alignment is presented.

In order to have precise track reconstruction it is essential to determine the exact positions of tracking detectors. For this purpose we have used the data taken with zero magnetic field, with and without a target.

1 No magnetic field, target out

The surveyed x positions of tracking detectors have been inspected using the run with zero magnetic field and without a target. Under these conditions the beam particles make straight track through the spectrometer. High voltages of DC2 and DC3 were lowered to have a clearer beam signal. The drift velocities ($v_{DC2} = 53.8\mu m/ns$ and $v_{DC3} = 51.2\mu m/ns$) remain the same since they are still in the saturation regime. The time offsets of the drift chambers have been re-determined using the raw TDC spectra for each wire hit by the beam particle.

Diagnosing the surveyed x positions, the beam tracks measured by the two BVERs and two drift chambers were fitted with a straight line. The position difference, δx, between the measured position x_{mea} and the linearly fitted position x_{fit} of x_{mea} at the surveyed z of each detector was calculated. Figure 1 shows δx's of the two BVERs, DC2 and DC3 for the surveyed values and corrections used in 1994.

There is large shift of these distributions from zero, thus the corrections to the surveyed x positions of the detectors made for 1994 data are no longer satisfying in 1995.

It should be noted that during this run the residual magnetic field was not quite zero. It is estimated to have been about 16 Gauss. The beam particles are still slightly deflected by this field, and according to the single bend and small angle approximation, the horizontal angle after the magnet is

$$\theta = \frac{0.29979\frac{Z_B}{A_B}BL}{p},$$

where p is the beam momentum measured in GeV/c, Z_B and A_B are charge and mass

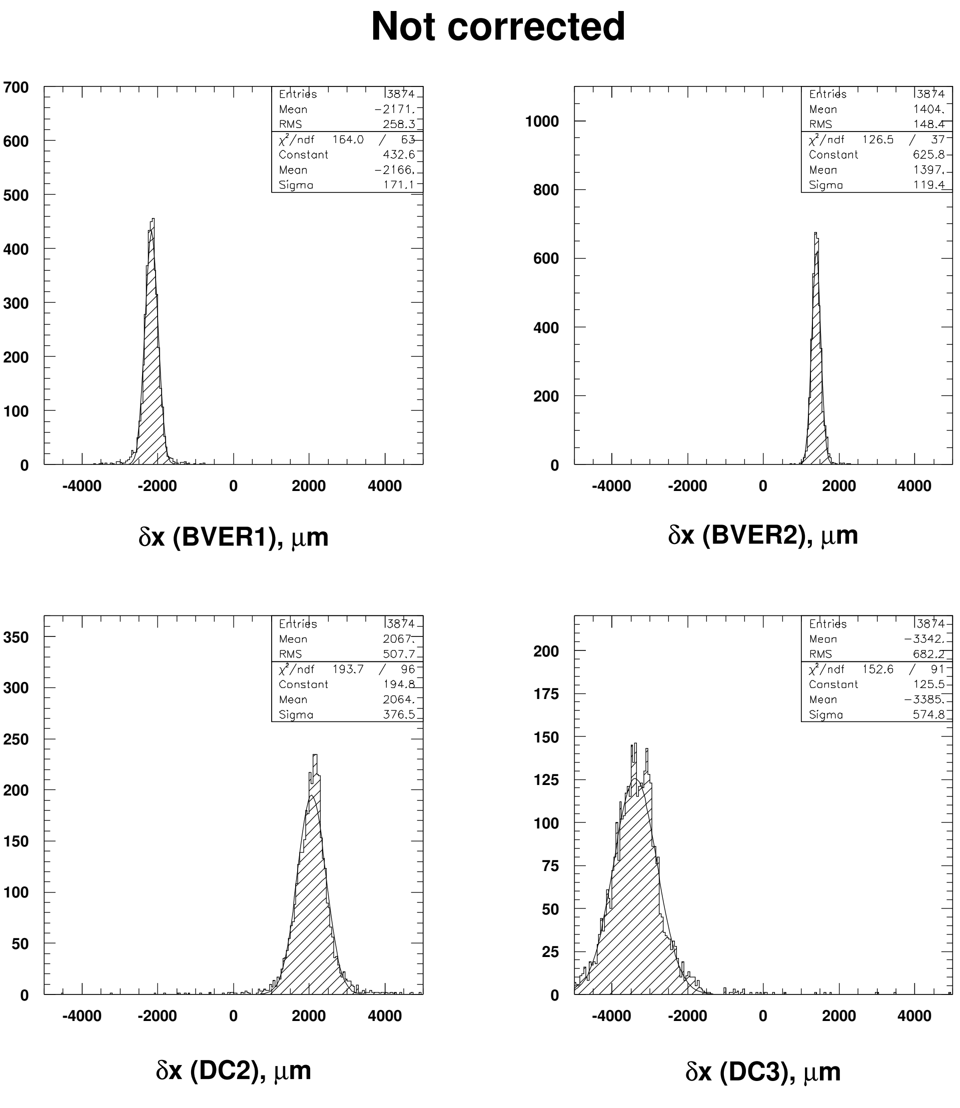

Figure 1: The difference between the measured position and fitted position δx for the two BVERs, DC2 and DC3 before 1995 corrections.

numbers of the beam particles, B is the magnetic field in Tesla and L is the effective length of the field.

Given that $B = 0.0016$ Tesla, $p = 11.4$ GeV/c, $L = 0.989$ m, $Z_B = 79$, $A_B = 197$, we obtain that for DC2 which is $z_{dc2} = 1830109\ \mu m$ away from the magnet, the systematic shift of x-coordinate $\Delta x = \theta z_{dc2}$ is 32 μm. For DC3 ($z_{dc3} = 7986421\ \mu m$), the systematic shift Δx is equal to 140 μm. These numbers despite being small are not quite negligible, so we take them into account before finding the offset corrections. The run prior to the zero field run was taken with B-field. In this field the positive beam particles are deflected to the right of the beam axis, which corresponds to the negative systematic shift in x position according to the E877 coordinate system. To compensate for this deflection, we have to shift all detectors after the magnet by the amount corresponding to the angle θ (140 μm for DC3). After aligning all detectors on the straight line, we re-adjust the correction factors back by the same amount.

To minimize the number of detectors to be moved, we have made an assumption that BVER1 and DC3 should stay in their places, and BVER2 and DC2 be shifted to get δx's centered at zero. The resulting histograms are presented in Figure 2.

The four MWPCs located in between DC2 and DC3 and used for track confirmation were also re-aligned. We have calculated the difference between measured x_{mea} position in MWPC and the x_{fit} position at the z of each MWPC given by the described above fit for each of four MWPCs before and after correction (Figure 3) . In track reconstruction algorithm, three out of four MWPCs are required for track to be confirmed. When MWPCs are not aligned (left panel of the figure), the probability of satisfying the above criteria is rather low, especially considering the small area where beam particles are traversing the spectrometer. It is indicated by the number of found beam tracks (3874 for 10000 beam triggers) and by the shape of the distributions. The right panel of (Figure 3) shows the difference between the measured position and fitted position after applying the correction factors given below. The shape of distributions is close to square with width corresponding to the wire spacing

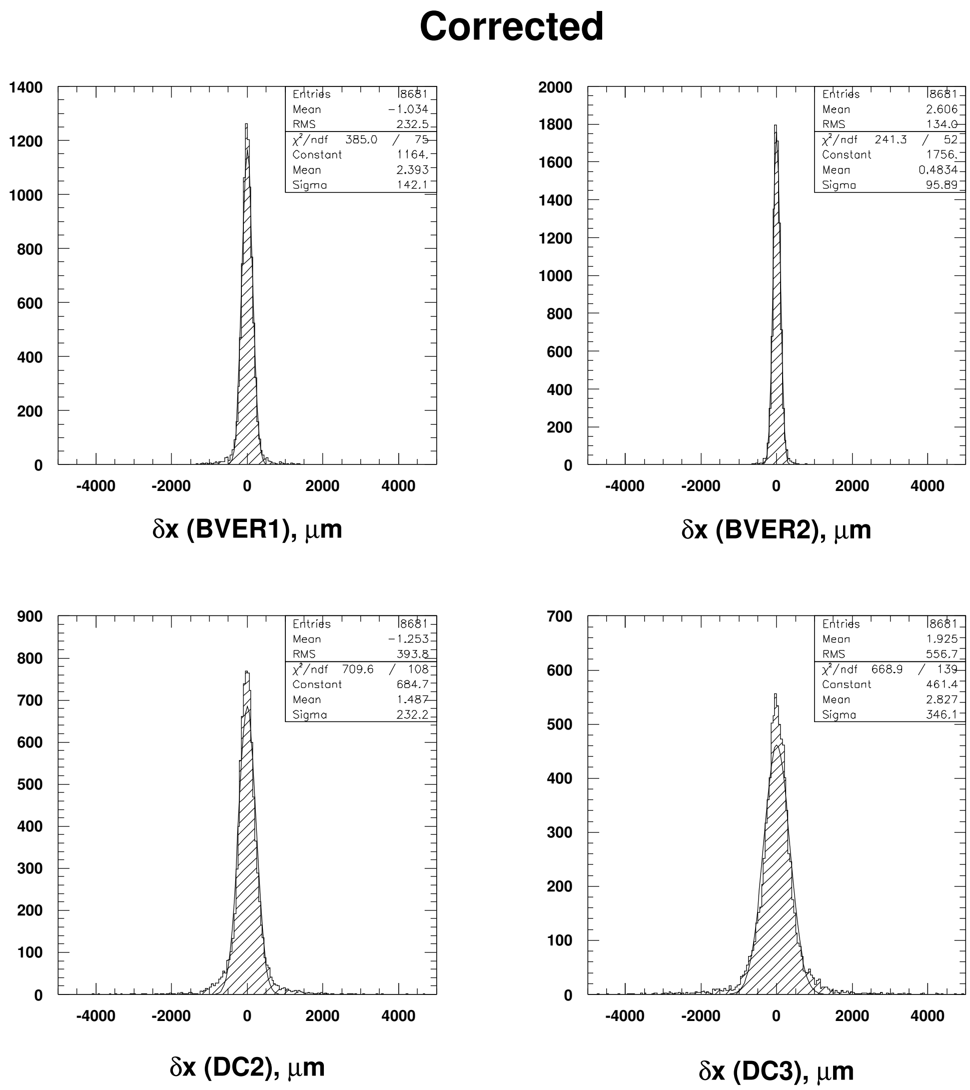

Figure 2: The difference between the measured position and fitted position δx for the two BVERs, DC2 and DC3 after corrections.

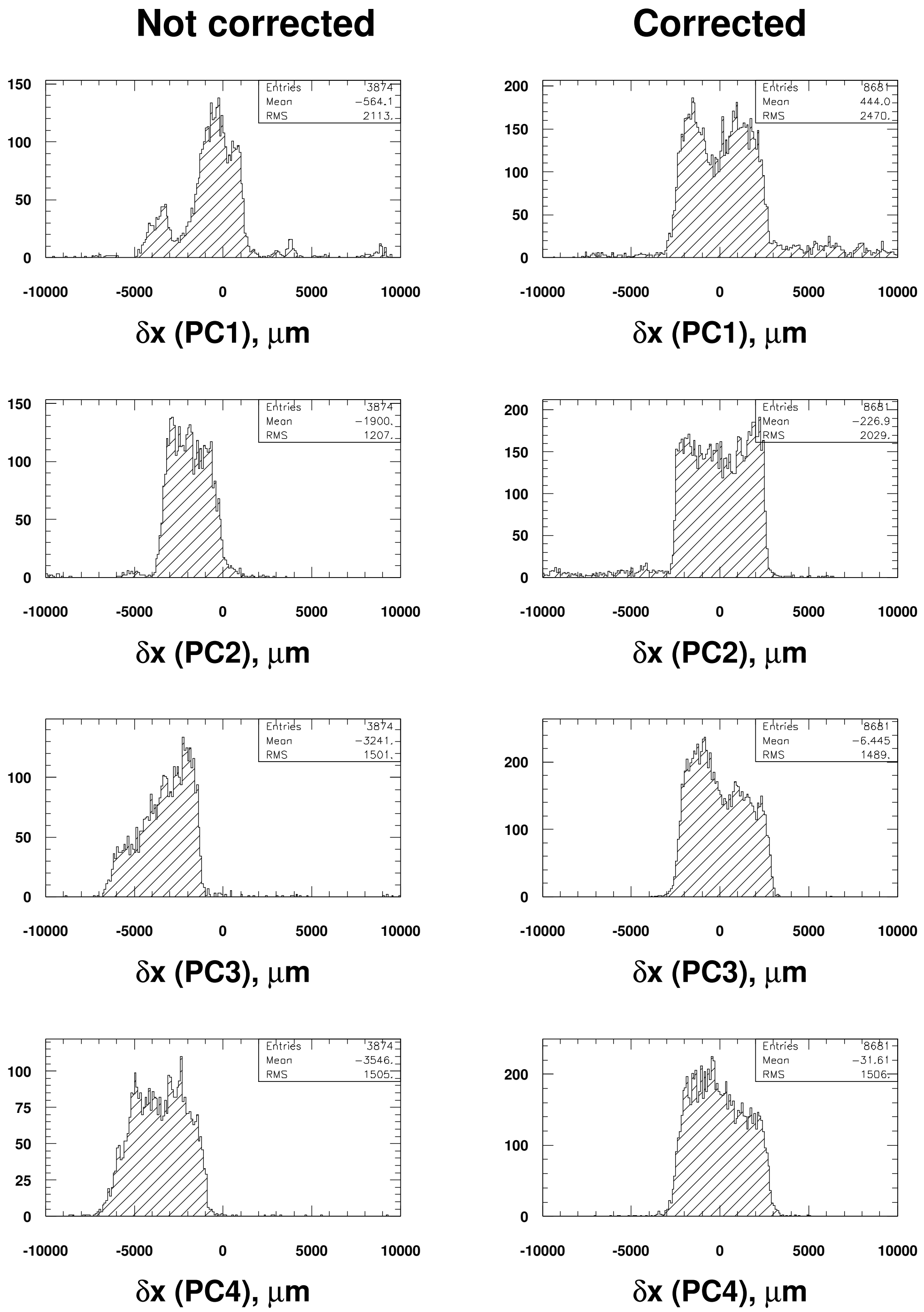

Figure 3: The difference between the measured position and fitted position δx for the four MWPCs before and after correction.

of MWPCs (5.08 mm). The number of found tracks has dramatically improved (8681 for 10000 beam triggers).

The surveyed positions and obtained correction factors are summarized in Table 1.

Table 1: The surveyed x positions, x_{survey}, and correction factors, $x_{correct}$ in microns for the 1994 and 1995 runs.

	z_{survey}, μm	x_{survey}, μm	$x_{correct}$, μm	
			1994 Run	1995 Run
BVER1	-5856000	0	351	0
BVER2	-2799000	0	-2813	-3723
DC2	5385200	222250	4781	-124
MWPC1	6632600	259060	1170	-208
MWPC2	7840600	289540	-894	-1602
MWPC3	9086900	320020	-1833	-587
MWPC4	10317200	350500	-1502	-493
DC3	111545875	380009	106	106

The correction factors given in the table are already adjusted to take into account the effect of small non-zero magnetic field.

2 No magnetic field, target in

To diagnose the surveyed z position of DC2 we have used the data with no magnetic field and a target. The run prior to that was taken with A-field. The time offsets of the drift chambers were re-calibrated for each wire (Figure 4).

Now we have a reaction, in which produced particles are emitted at various angles and travel without bending in zero magnetic field. The resulting straight tracks measured by the drift chambers should be pointing to the initial position of interaction

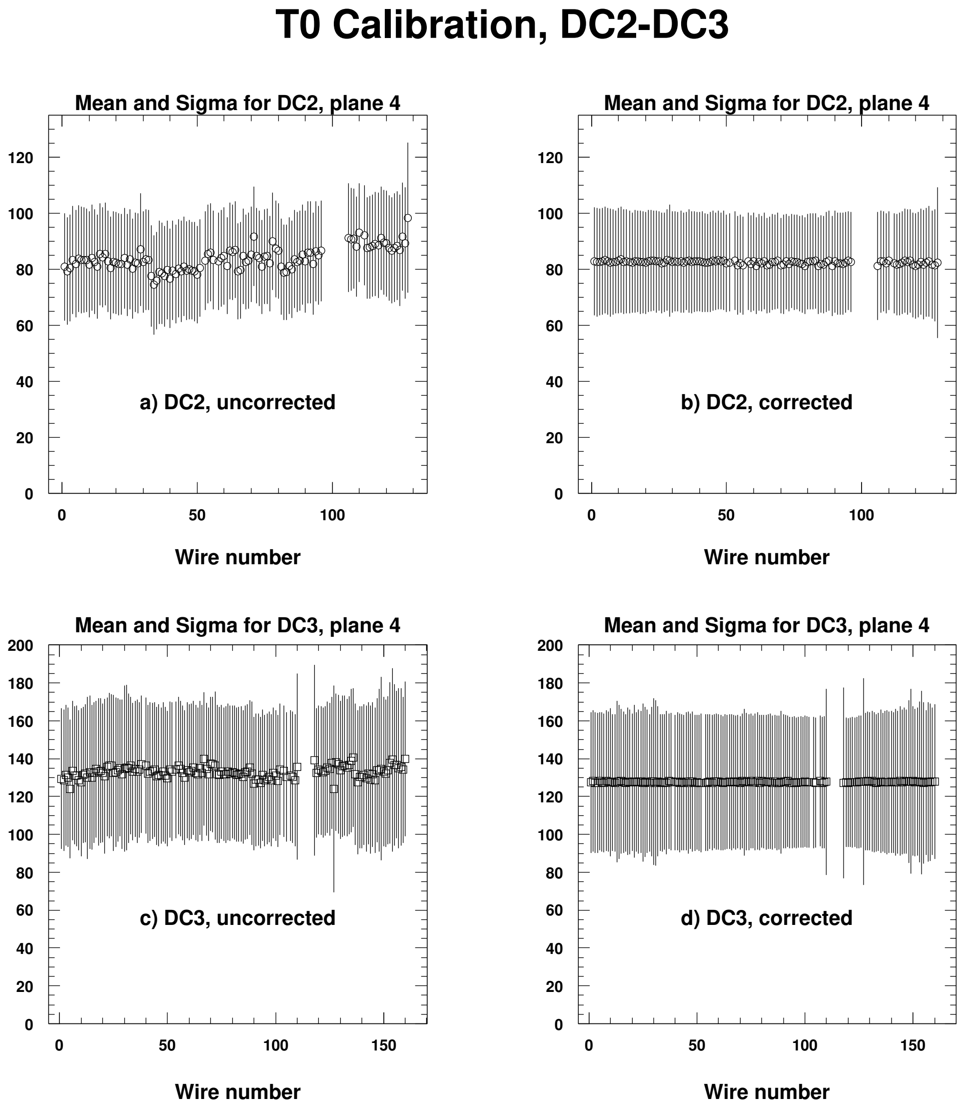

Figure 4: The time offsets of DC2 and DC3 before calibration (left panel) and after (right panel).

at the target, which is measured by the beam vertex detectors. By examining the difference between the x position of beam particles at the target measured by the BVERs and the x position of tracks projected back to the target measured by the DCs we can find the optimum z position of DC2. If DC2 is in the right place, the particles produced in the reaction should be focused at $z = 0$ (target position), and the width of the distribution would be minimal. Figure 5 shows this distribution for the surveyed z position of DC2 after applying x corrections found before.

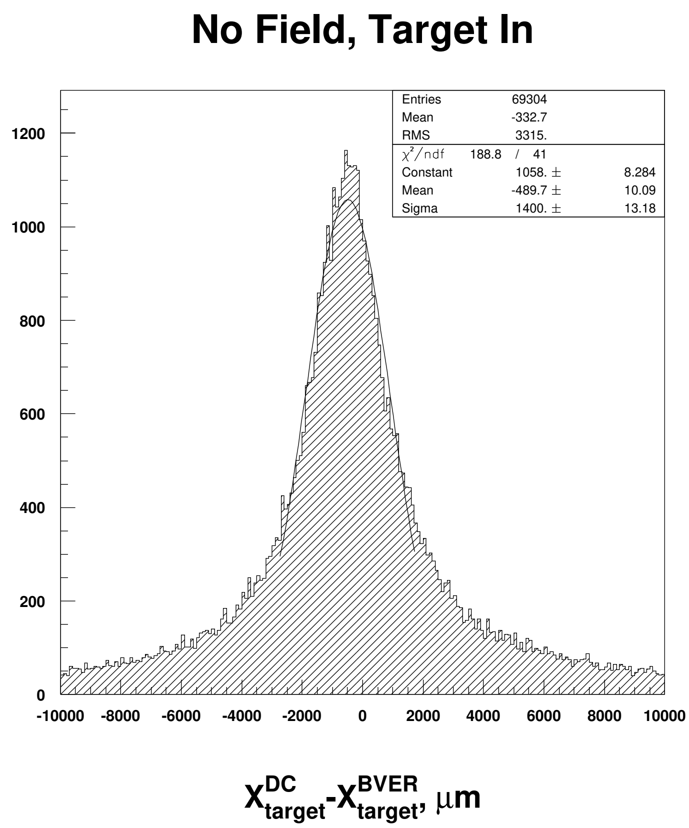

Figure 5: The difference between the x positions on the target given by the DCs and the BVERs for the $z_{DC2}^{survey} = 538.52$ cm after corrections

Varying the z position of DC2 changes the peak position and the width of the distribution. It is illustrated in Figure 6, where σ of Gaussian fit is plotted for different values of z_{DC2}. The minimum of a parabolic fit has been achieved for $z_{DC2} = 538.266$

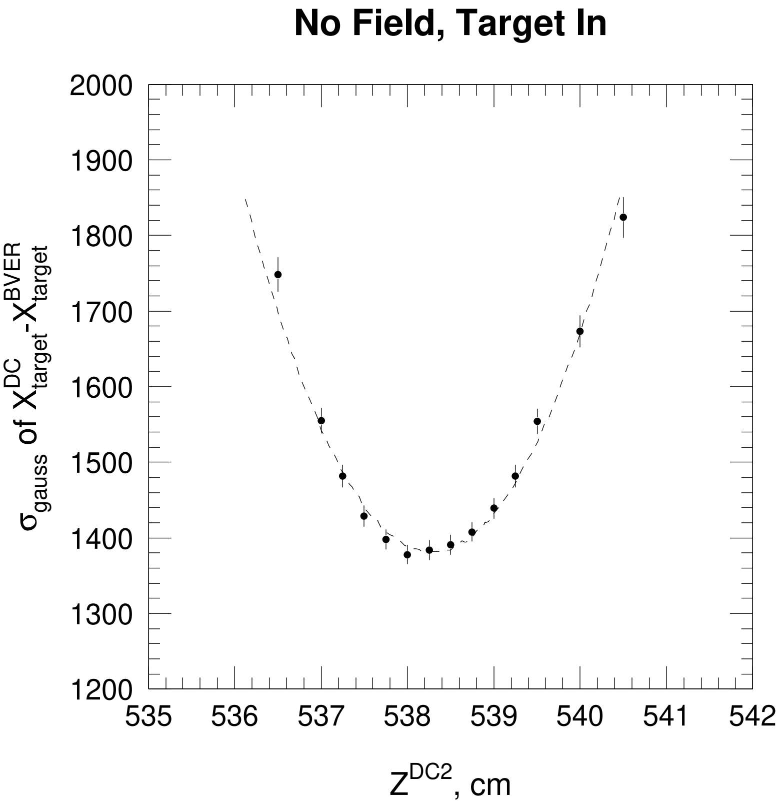

Figure 6: The width (σ_{gauss}) of distribution of the difference between the x positions on the target given by the DCs and the BVERs for different values of z position of DC2.

cm. For this position, the peak of distribution shown in Figure 6 is at -660 microns, which is consistent with bending of positive particles of momentum 2.7 GeV/c in 16 Gauss A-field.

We can test how well the obtained correction factors work for the run with a target by employing similar procedure we have used to find the offset corrections. Two measurements done by BVERs provide us with precise x position of the beam on target, or, the origin of all particles produced in an interaction. Thus, three x

positions, the x_{target} position obtained from BVERs and the two x positions of each particle measured by the DCs, may be fitted by a straight line. The difference δx between the measured position and position of the line of fit at z of each detector is plotted in Figure 7 for BVER, TOFU, DC2 and DC3.

The peak of each distribution is within 200 microns of zero. The shape of TOFU distribution corresponds to the two different widths of TOFU slats, 1.7 cm and 1 cm. The tails are most likely due to multiple scattering and low momenta particles bent by small non-zero magnetic field.

The further study has shown that δx slightly depends on the measured position, which is illustrated in Figure 8. This effect could be due to several reasons, such as misalignment in z or a slight "tilt" of DC2 and/or DC3, small residual magnetic field, non-zero thickness of the target, etc.

3 Magnetic field, target in

The correction factors have also been tested with real data run by looking at the mass spectra. The following two figures were obtained by Yi Dai for x corrections given in Table 1 and $z_{DC2} = 538.52$ cm. Figure 9 presents the distribution of momentum squared versus mass squared for protons and pions. The dependence of mass on momentum squared is shown in Figure 10. The reconstructed mass of proton is 929.38 MeV/c with very slight dependence on momentum.

We have also estimated the tracking efficiency before and after corrections. Using the event display, for each event we recorded the number of reconstructed tracks and the number of missed tracks which were visible by eye. If one takes the number of reconstructed tracks plus the number of missed tracks as 100%, then the number of reconstructed tracks before corrections is about 54%, and the number of reconstructed tracks after applying alignment corrections is about 81%. Although the absolute numbers are somewhat subjective, there is a significant improvement in tracking

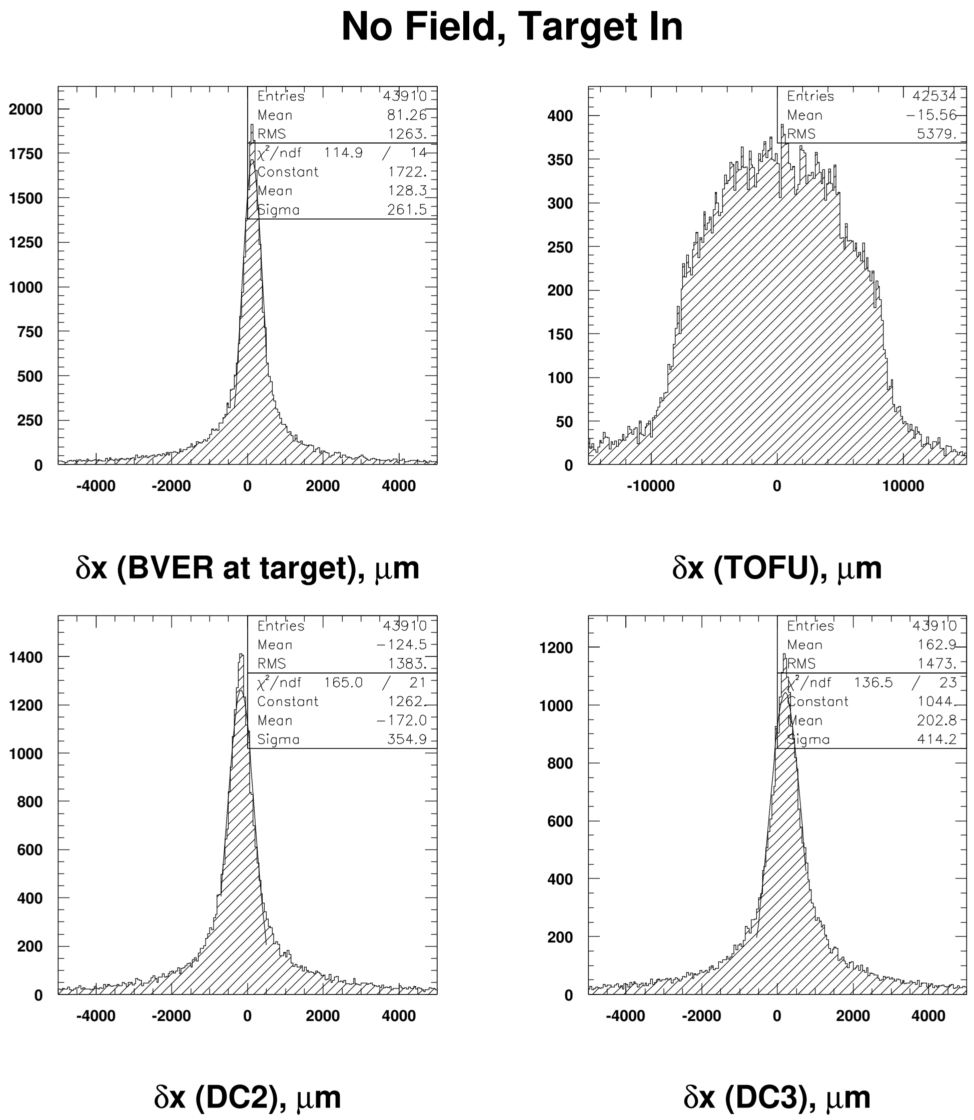

Figure 7: The difference between the measured position and fitted position δx for the BVER, TOFU, DC2 and DC3 after corrections.

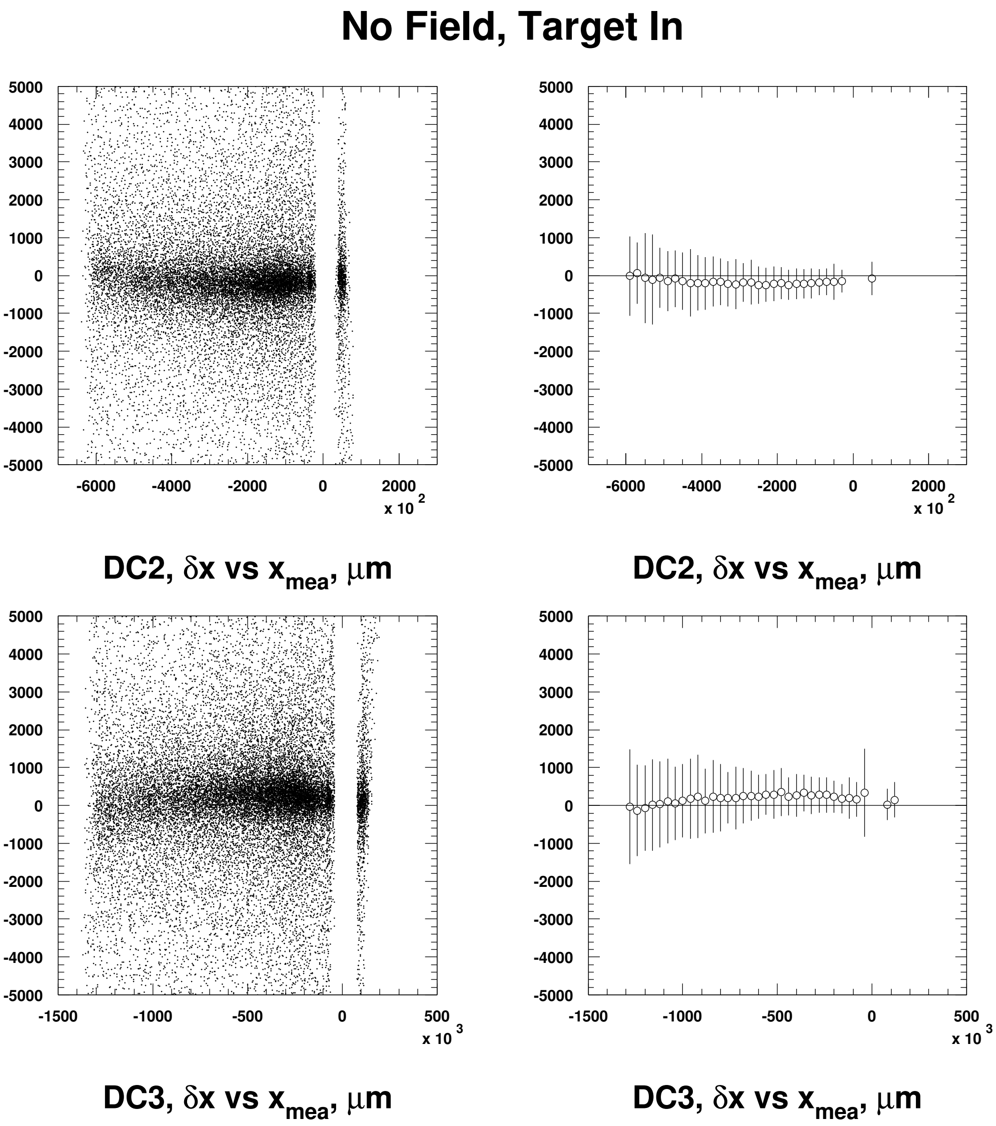

Figure 8: The difference between the measured position and fitted position δx as function of measured position for DC2 and DC3 after corrections.

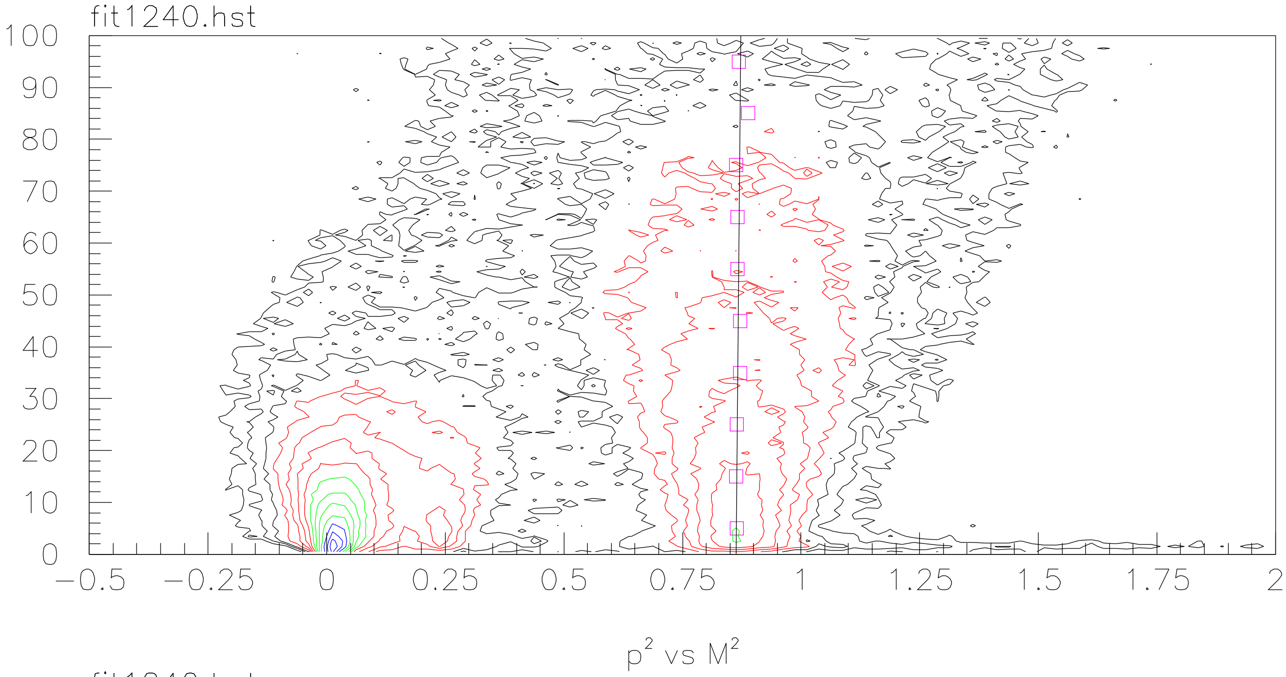

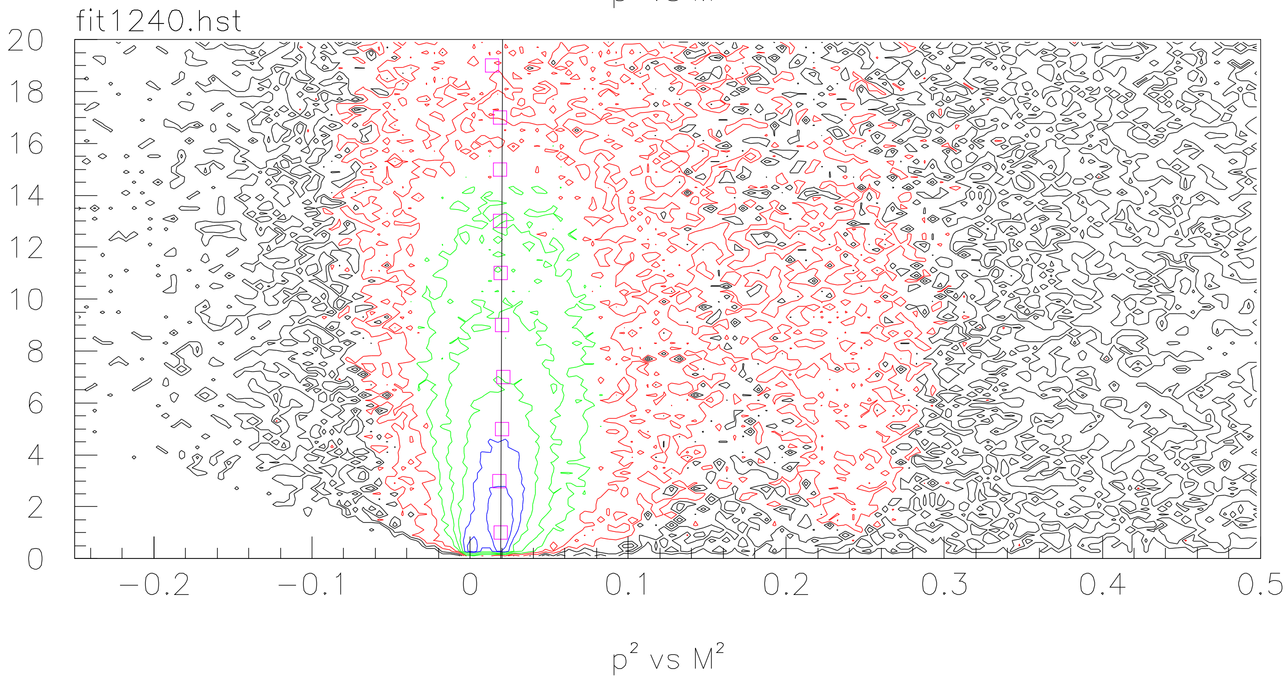

Figure 9: The mass squared versus momentum squared for protons (upper plot) and pions (lower plot).

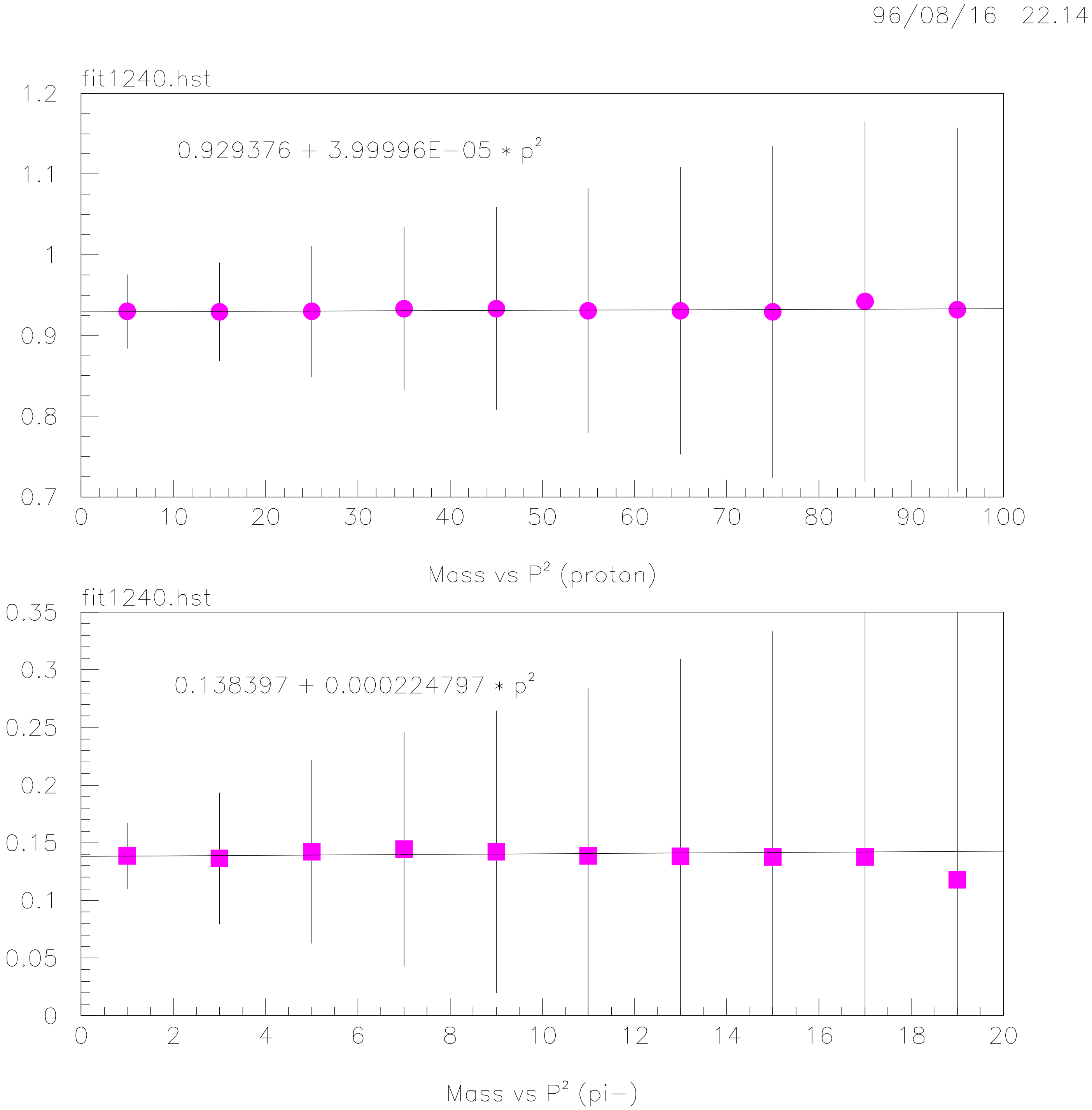

Figure 10: The mass versus momentum squared for protons (upper plot) and pions (lower plot).

efficiency after the spectrometer alignment.

4 Alignment of drift chambers in y.

The beam particles run cannot be used for y alignment due to the dead beam region of DC2 and DC3 pad planes. Therefore the drift chambers have been aligned in the y direction using the real data run. A precise y position of beam at target provided by the beam vertex detectors and y positions measured by the DC2 and DC3 pad planes were fitted by a straight line. The difference between the measured position and fitted position δy for the BVER, TOFU, DC2 and DC3 after moving DC2 by -1910 microns in y direction is plotted in Figure 11.

Since the error in y position measured by the BVER detectors is much smaller than that measured by the drift chambers (200 microns for BVERs compared to 4000-6000 microns for DCs), the fit is always close to the y position given by the BVERs. This results in a very narrow distribution of BVER's δy. Although we have not used y positions measured by the TOFU in fitting, the mean of TOFU's δy distribution is very close to zero. The correction of y position of DC2 by -1910 μm is sufficient to get all δy's centered at zero.

5 Alignment of vertex chambers.

After aligning detectors used in tracking algorithm, clusters in the two vertex chambers (VTXA, VTXB) placed before the magnet need to be aligned with the back projections of the downstream tracks. For this purpose we have used distributions of the distances Δx and Δy between each track and its closest cluster. Figure 12 shows raw close cluster distributions in x and y for both vertex detectors. The non-zero means are the result of chamber misalignment.

Before finding the offset corrections for x and y, z positions of the chambers

Corrected

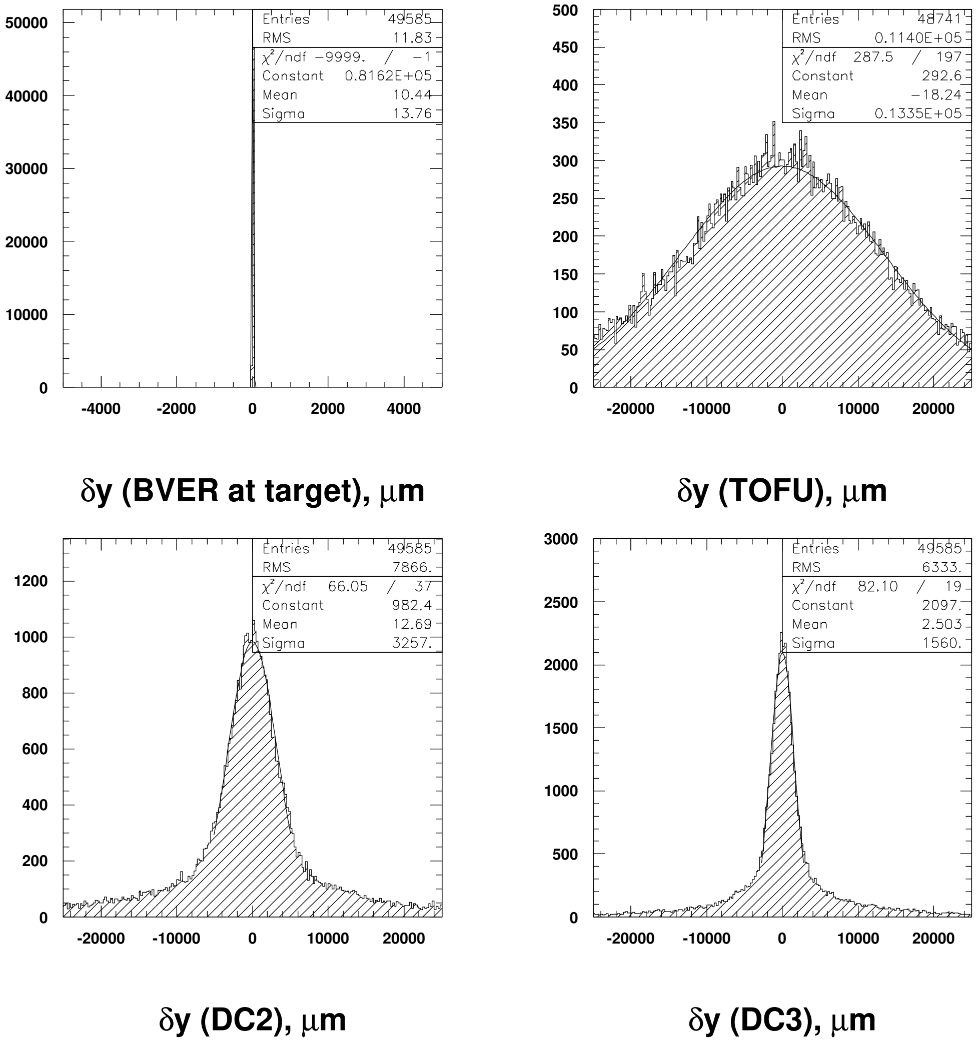

Figure 11: The difference between the measured position and fitted position δy for the BVER, TOFU, DC2 and DC3 after corrections.

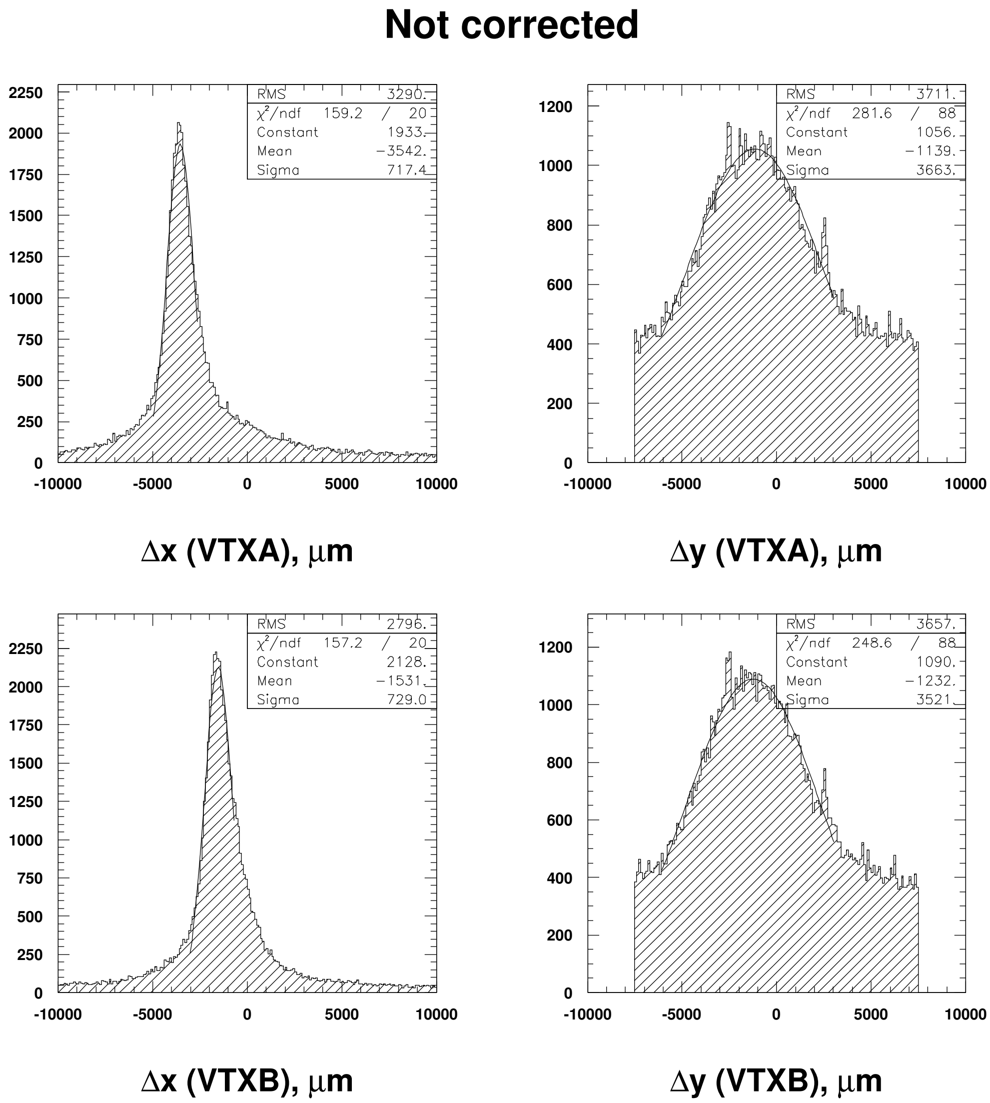

Figure 12: Raw close cluster distributions, in x and y, for both vertex detectors before corrections.

need to be determined. The dependance of Δx on the measured x position shown in Figure 13 for both vertex chambers indicates that the z positions of VTXA and VTXB ought to be adjusted. The strong linear position dependance diminishes after correcting detectors' z position (Figure 14).

Corrected raw close cluster distributions for both vertex chambers are presented in Figure 15. The determined z positions and correction factors for vertex chambers are given in Table 2.

Table 2: The z positions and correction factors for vertex chambers in microns for 1994 and 1995 run.

Run	Detector	z	$x_{correct}$	$y_{correct}$
1994	VTXA	2005000	0	-2000
	VTXB	2255000	0	-2000
1995	VTXA	2017750	-4118	-3565
	VTXB	2271000	-2239	-3633

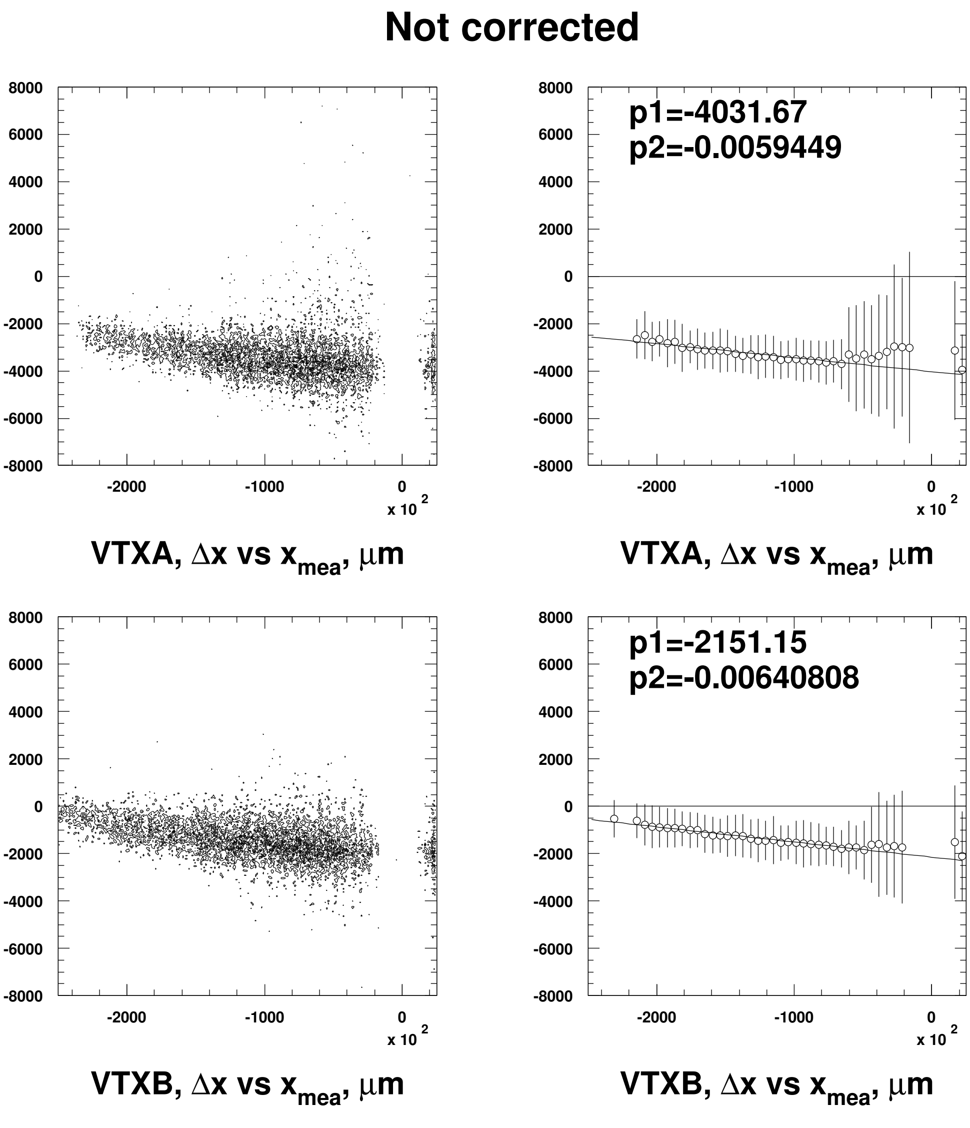

Figure 13: The dependance of the x distance between track and its closest cluster (Δx) on the x position of the cluster for VTXA, VTXB before corrections. p1, p2 are parameters of fit by a straight line.

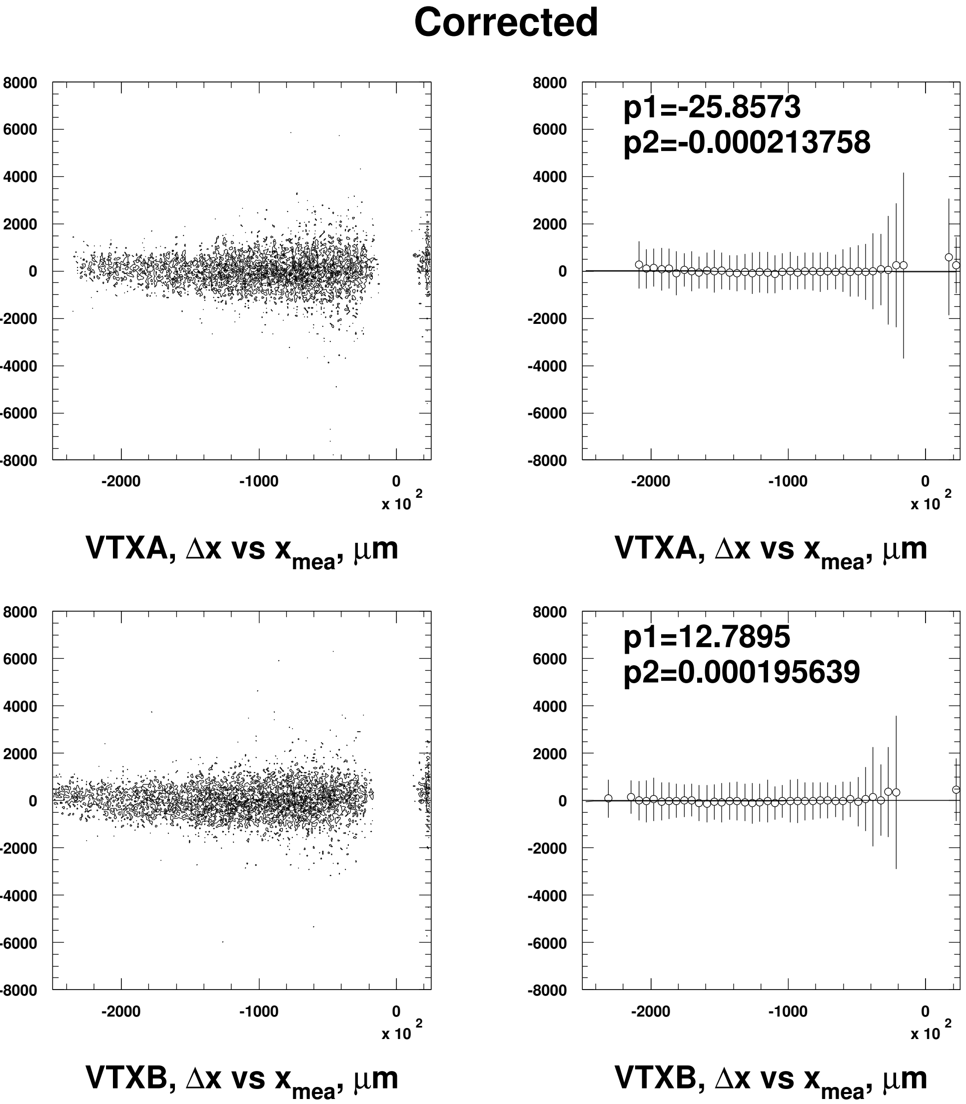

Figure 14: The dependance of the x distance between track and its closest cluster (Δx) on the x position of the cluster for VTXA,VTXB after corrections. p1, p2 are parameters of fit by a straight line.

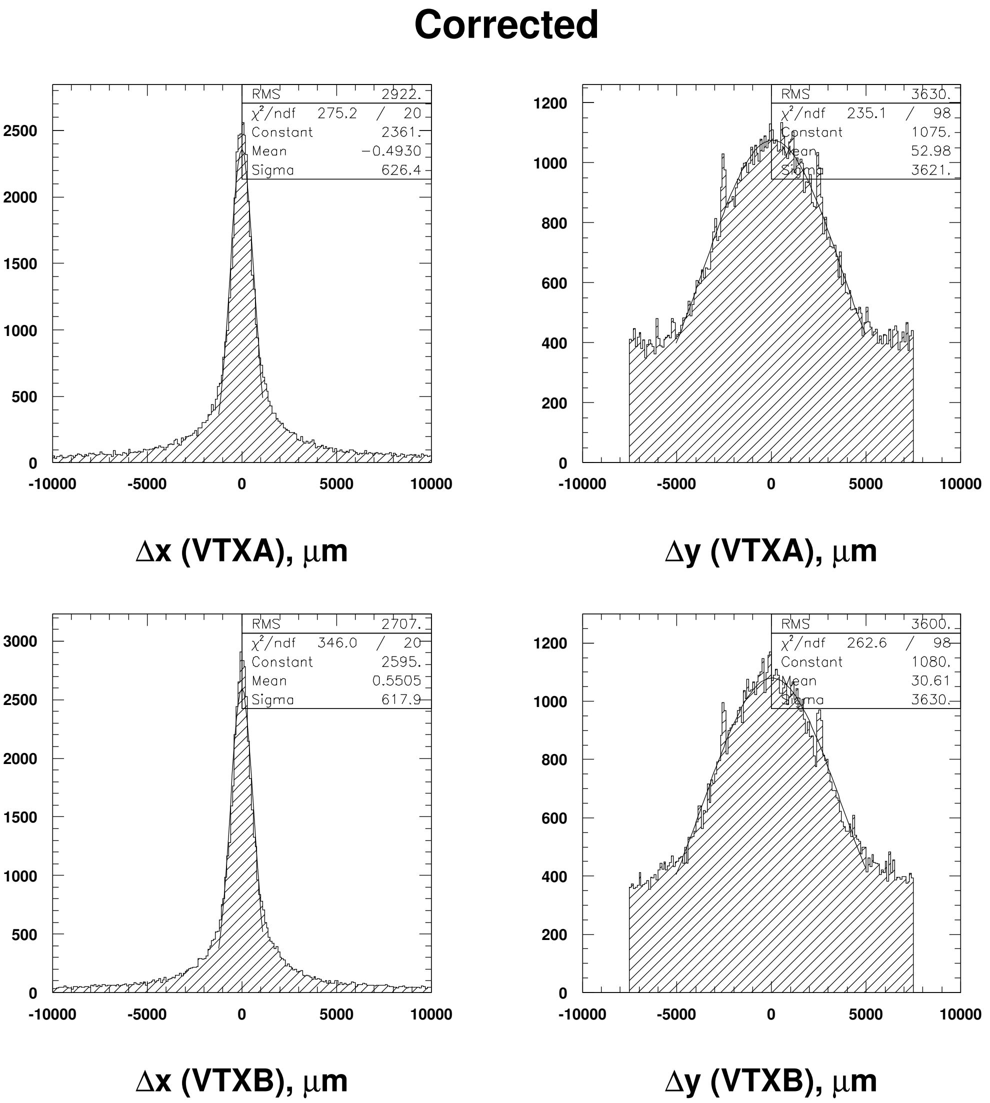

Figure 15: Raw close cluster distributions, in x and y, for both vertex detectors after corrections.

Appendix

A Summary of results

The parameters of 1994 and 1995 alignment are given in Table 3.

Table 3: The parameters of 1994 and 1995 alignment.

Detector	Parameter	1994 value	1995 value
BVER1	V1_SRVX_CORR	351	0
BVER2	V2_SRVX_CORR	-2813	-3723
VTXA	VTXA_Z	2005000	2017750
	VTXA_SRVX_CORR	0	-4118
	VTXA_SRVY_CORR	-2000	-3565
VTXB	VTXB_Z	2255000	2271000
	VTXB_SRVX_CORR	0	-2239
	VTXB_SRVY_CORR	-2000	-3633
DC2	DCII_SRV_Z	5385200	5382660
	DCII_SRVX_CORR	4781	-124
	DCII_SRVY_CORR	0	-1910
MWPC1	PCI_SRVX_CORR	1170	-208
MWPC2	PCII_SRVX_CORR	-894	-1602
MWPC3	PCIII_SRVX_CORR	-1833	-587
MWPC4	PCIV_SRVX_CORR	-1502	-493